A study of the ^{16}O(e,e$'$p) reaction at deep missing energies

ROUGH DRAFT
(April 2, 1999)

The ^{16}O(e,e$'$p) reaction was studied in the quasielastic region at $q = 1000$ MeV and $\omega = 445$ MeV. R_L, R_T and R_{LT} response functions were extracted for $25 < E_{miss} < 60$ MeV and $P_{miss} < 280$ MeV/c.

At lower p_{miss} ($p_{miss} < 150$ MeV/c), R_L and R_T are mostly accounted for by the DWIA and HF-RPA models of s-shell knockout for $E_{miss} < 50$ MeV. For $E_{miss} > 50$ MeV , R_T remains strong while R_L appears to go to zero. At $p_{miss} \approx 280$ MeV/c R_L is consistent with zero and with theory. R_T and R_{LT} are much bigger than the DWIA calculation but the same size as the HF-RPA calculation.

The coincidence (e,e$'$p) reaction in quasielastic kinematics ($\omega = q_\mu^2/2m_p$ where q_μ and ω are the four-momentum and energy transfers) has long been a crucial tool in the study of nuclear structure. (e,e$'$p) cross section measurements have provided a wealth of information on the wave functions of the protons inside the nucleus and have provided stringent tests of nuclear theories. Response function measurements have provided detailed information about the different reaction channels contributing to the cross section such as single- and multi-nucleon knockout, meson exchange currents, isobar excitations, and final state interactions.

Originally, the quasielastic cross-section was attributed entirely to single particle knockout from valence states of the nucleus. However, a series of ^{12}C(e,e$'$p) experiments performed at MIT-Bates [2], [3], [4] [5], [6] [7], [8] which sampled various kinematic regions measured much larger cross sections at high missing energy ($E_{miss} = \omega - T_p$ where T_p is the final proton kinetic energy) than was expected for single particle knockout. Separated C(e,e$'$p) coincidence data reported by Ulmer *et alia* [2] show a dramatic increase in the transverse-to-longitudinal ratio above the two-particle emission threshold. This enhancement indicates the presence of an additional, transverse, nonquasielastic reaction mechanism. The longitudinal response becomes consistent with zero above $E_{miss} = 50$ MeV, indicating that single particle knockout is very small above this point. Similar R_T/R_L enhancement has been observed at NIKHEF-K for ^{6}Li [28] and ^{12}C [29]. These findings indicate that a large part of the cross section at large missing energies comes from two-body and multi-body processes.

There have been several theoretical attempts to explain the continuum strength using many-body knockout models, but no model can explain all the data [10], [14]. It has also been suggested that short-range and tensor correlations could play a major role in populating the high E_{miss} continuum. Muther *et al.* [15] calculated the effects of these correlations in ^{16}O and have shown that they shift strength from conventional quasi-hole states to high-E_{miss}, high-P_{miss} channels.

In this experiment we measured the ^{16}O(e,e$'$p) reaction in the quasielastic region at $|\vec{q}| = 1000$ MeV and $\omega = 445$ MeV. We extracted the longitudinal (R_L), transverse (R_T) and longitudinal-transverse (R_{LT}) response functions from cross sections measured at several beam energies (E_0) and electron angles (θ_e) for $E_{miss} < 60$ MeV and $P_{miss} < 280$ MeV/c. This was the first Jefferson Lab Hall A experiment and the first response function separation on a complex nucleus at large (P_{miss}, E_{miss}). This paper reports the results for $E_{miss} > 25$ MeV.

We scattered the continuous incident electron beam from a waterfall target [17] and detected the scattered electrons in the High Resolution Electron Spectrometer (HRS$_e$) and the protons in the High Resolution Hadron Spectrometer (HRS$_h$) [21]. The HRS$_e$ detector package consisted of two scintillator planes to generate the trigger, a gas Cherenkov detector for particle identification and a pair of two-plane Vertical Drift Chambers (VDCs) for trajectory determination. Only the HRS$_h$ VDCs and trigger scintillators were used for this experiment.

The waterfall target consisted of three flat flowing water 'foils', each approximately 130 mg/cm^2 thick along the beam and at 30° to the incident beam. Using three foils improved our target energy loss determination and allowed us to use vertex cuts to reject accidentals.

We measured the ^{16}O(e,e$'$p) cross-sections at three beam energies, 0.843, 1.643 and 2.442 GeV, keeping $|\vec{q}|$ and ω fixed, in order to vary the virtual photon polarization. At 0.843 and 1.643 GeV, we measured the cross section for three different proton-virtual photon angles, $\theta_{pq} = 0°, \pm 8°$. At 2.442 GeV, we measured at $\theta_{pq} = 0°, \pm 8°, \pm 16°$. See table details. This allowed us to separate R_L and R_T at $\theta_{pq} = 0°$ and $R_L + \frac{V_{TT}}{V_L} R_{TT}, R_T$ and R_{LT} at $\theta_{pq} = 8°$ and 16° with some redundancy for checking our systematic uncertainties.

The accuracy of a response function separation depends on matching the values of $|\vec{q}|$ and ω between different kinematic settings with different virtual photon polarizations. In order to match $|\vec{q}|$ and locate $\vec{q}$, we measured H(e,e$'$p) (also present in the waterfall target) with a pin-hole collimator on HRS$_e$. The momentum of the detected protons is equal to $\vec{q}$. We determined the location of the H(e,e$'$p) momentum peak to $\frac{\delta p}{p} = 2 \times 10^{-4}$ allowing us to match $|\vec{q}|$ to 2×10^{-4} between different kinematic settings. Throughout the experiment H(e,e$'$) data, measured simultaneously with the ^{16}O(e,e$'$p) data from the waterfall target, provided a continuous monitor of luminosity and beam energy.

We binned the data in the four dimensional ω, Q^2, E_{miss}, and P_{miss} space. The six-fold differential cross section for a bin $B(\omega,\, Q^2,\, E_{miss}, P_{miss})$ can be expressed by

$$\frac{d^6\sigma}{d\omega d\Omega_e dE_p d\Omega_p} = \frac{N_B}{L\varepsilon_e\varepsilon_p\varepsilon_{coin}V_B} D R_B, \qquad (1)$$

where
N_B is the number of particles scattered into the bin $B(\omega,\, Q^2,\, E_{miss},\, P_{miss})$,
L is the luminosity,
ε_e and ε_p are the electron and hadron spectrometer efficiencies, and ε_{coin} is the coincidence trigger efficiency,
V_B is the phase space volume of the bin,
D is the dead-time correction, and
R_B is the radiative correction.

We determined the product $L\varepsilon_e$ by normalizing the measured H(e,e$'$) cross section to a parameterization [18] of the world data. We calculated the phase space volume for each bin (V_B) using a Monte-Carlo simulation. We determined the product $\varepsilon_p\varepsilon_{coin}$ using the ratio of simultaneously measured H(e,e$'$p) to H(e,e$'$) cross-sections. We calculated the radiation correction factor R_B for each bin using the code RADCOR [19], [20], [21] which unfolds the radiative tails in the E_{miss} P_{miss} space.

In the first Born approximation the non-polarized (e,e$'$p) cross section can be expressed as [1]

$$\frac{d^6\sigma}{d\Omega_e d\Omega_p d\omega dE_{p'}} = \frac{p' E_{p'}}{(2\pi)^3}\sigma_{Mott}(V_L R_L + V_T R_T + V_{LT} R_{LT}\cos\phi + V_{TT} R_{TT}\cos 2\phi), \qquad (2)$$

where V_L, V_T, V_{LT} and V_{TT} are kinematic factors only dependent on the electron vertex, ϕ is the angle between the electron scattering plane and the reaction plane, and σ_{Mott} is the Mott cross section.

In parallel kinematics, because the out-of-plane angle ϕ is not defined only $R_{\rm L}$ and $R_{\rm T}$ survive in the expression for the cross section. The Rosenbluth method may be used to separate R_L and R_T. In the case of perpendicular kinematics, all four terms are present in the expression for the cross section. By measuring the cross section on both sides of $\vec{q}$ ($\phi = 0°$ and $\phi = 180°$) keeping all other kinematic variables constant, $R_{\rm LT}$ can be extracted according to

$$R_{LT} = \frac{(2\pi)^3}{E_p p_p \sigma_M}\left[\frac{\sigma(0°) - \sigma(180°)}{2V_{LT}}\right] \qquad (3)$$

The separation of $R_{\rm TT}$ requires an out-of-plane measurement. An in-plane Rosenbluth separation in the case of perpendicular kinematics allows for the separation of $R_L + \frac{V_{TT}}{V_L}R_{TT}$ and R_T.

For the "parallel" kinematic setting of this experiment ($\theta_{pq} = 0°$) the H(e,e$'$p) peak and the associated radiative tail were present in the coincidence phase-space for ^{16}O. To remove H(e,e$'$p) events we cut out all events with $P_{miss} < 45$ MeV/c. This cut significantly reduced the ^{16}O(e,e$'$p) statistics for this setting. This cut removed a large fraction of the events with $\vec{P}_{miss} \parallel \vec{q}$. However, since the remaining events have $\vec{P}_{miss}$ symmetrically distributed around $\vec{q}$, this data sample is approximately parallel, in that the interference response functions, which are dependent on ϕ (the azimuthal angle around $\vec{q}$), average out to zero. Due to this problem we call this setting "quasi-parallel" kinematics. The perpendicular kinematic settings had no contamination due to H.

Figs. 1- 3 present the separated response functions from this experiment for $|\theta_{pq}| = 0, 8°$ and $16°$ corresponding to missing momenta of approximately 60, 145 and 280 MeV/c. Note that 280 MeV/c is larger than the fermi momentum of oxygen, $p_F \approx 220$ MeV/c.

In order to check how much of the observed continuum strength can be explained by $1s_{1/2}$ knockout, we compared our results to $1s_{1/2}$ single particle knockout calculations by Van Orden [24], [25], Kelly [1] and Ryckebusch [11], [12], [13]. The Ryckebusch calculations (Impulse Approximation (IA) calculations and calculations that include two-body current contributions related to Meson Exchange Currents (MECs) and Δ-creation) have been performed in a self-consistent Hartree-Fock (HF), Random Phase Approximation (RPA) frame work. Kelly calculations are non-relativistic DWIA (Distorted Wave Impulse Approximation) calculations while Van Orden calculations relativistic DWIA.

We distributed the calculated $1s_{1/2}$ response functions in E_{miss} using a prescription given by Jeukenne and Mahaux [22], [10], where the $1s_{1/2}$ profile is modeled using a Lorentzian with an energy-dependent width $\Gamma(E)$. This shape described the $p_{miss} \approx 60$ MeV/c data well (see Fig.1) but did not describe the higher p_{miss} data well.

Fig. 1 presents the separated response functions for the "quasi-parallel" kinematic setting. The wide bump centered around $E_{miss} = 40$ MeV in both R_L and R_T corresponds primarily to single particle knockout from the $1s_{1/2}$ state. The difference between the transverse and longitudinal spectral functions ($S_T - S_L$), which is expected to be zero for a free nucleon, is nonzero for $E_{miss} > 40$ MeV and is about half the size of the spectral function difference measured on carbon at $q = 400$ MeV/c [2]. This might indicate that the non-single particle knockout mechanisms responsible for the $L-T$ difference decrease faster with q than the nucleon formfactors. The errors on $S_T - S_L$ are too large to draw any conclusions about the onset of the difference.

Fig. 2 presents the separated response functions for the $|\theta_{pq}| = 8°$ perpendicular kinematic setting, ($p_{miss} \approx 145$ MeV/c). At this point R_T is approximately constant for the entire range of missing energy measured ($25 < E_{miss} < 60$ MeV) whereas $R_L + V_{TT}R_{TT}/V_L$ becomes consistent with zero for $E_{miss} > 50$ MeV. Since $\frac{V_{TT}}{V_L}R_{TT}$ is estimated to be about 7% of R_L, this behavior can be attributed mainly to R_L. R_{LT} peaks at about 40 MeV but is always negative, indicating that R_L is not zero. R_{LT} is about one-third the size of R_T. The Mahaux parametrization does not reproduce the missing energy shape of R_L or R_T.

All four calculations underestimate the measured R_{LT} over the whole range of E_{miss}. As in the case of quasi-parallel kinematics, the inclusion of MEC+Δ in the HF-RPA calculation seems to bring it closer to the data (and to the relativistic DWIA calculation). For $E_{miss} < 35$ MeV, all response functions are larger than the calculations. For $E_{miss} > 50$ MeV, $R_L + \frac{V_{TT}}{V_L}R_{TT}$ is consistent with both zero and the calculations. R_T, on the other hand, appears to retain strength above 50 MeV. This is in agreement with the high E_{miss} behavior of R_L and R_T observed in parallel kinematics during the present experiment and also at MIT-Bates by Ulmer *et al.* [2], [3].

Fig. 3 presents the separated response functions for the $|\theta_{pq}| = 16°$ perpendicular kinematic setting, $p_{miss} \approx 280$ MeV/c. At this point, R_T and R_{LT} appear to slowly decrease over $25 < E_{miss} < 60$ MeV whereas $R_L + V_{TT}R_{TT}/V_L$ is consistent with zero. R_{LT} is about one-third the size of R_T. The shapes of R_T and R_{LT} are not consistent with Mahaux's parametrization.

At $p_{miss} \approx 280$ MeV/c, the total HF-RPA calculation predicts much higher strength for all the response functions than the DWIA calculations. This might be due to the fact that the HF-RPA calculation accounts for long range correlations in the RPA framework while the DWIA calculations do not. R_L is close to zero as expected by all three calculations. However, R_T and R_{LT} are much larger than the DWIA calculation and approximately as large as the HF-RPA calculation. Neither R_T nor R_{LT} show a peak at $E_{miss} \approx 40$ MeV corresponding to single particle knockout from the s-shell.

In summary, for $45 < p_{miss} < 75$ MeV/c, R_L and R_T are close to DWIA and HF-RPA models of s-shell knockout. The difference between the transverse and longitudinal spectral functions ($S_T - S_L$), which is expected to be zero for a free nucleon, is nonzero for $E_{miss} > 40$ MeV and is about half the size of the spectral function difference measured on carbon at $q = 400$ MeV/c [2]. This might indicate that the non-single particle knockout mechanisms responsible for the $L - T$ difference decrease faster with q than the nucleon form factors. At $p_{miss} \sim 150$ MeV/c R_L and R_T are mostly accounted for by the DWIA and HF-RPA models of s-shell knockout for $E_{miss} < 50$ MeV. For $E_{miss} > 50$ MeV, R_T remains strong while R_L appears to go to zero. At $p_{miss} \approx 280$ MeV/c R_L is consistent with zero and with theory. R_T and R_{LT} are sinnificuntly bigger than the DWIA prediction but are comparable to the HF-RPA calculations.

[1] J.J. Kelly, Adv. Nucl. Phys., **23** ed. by J.W. Negele and E. Vogt 75 (1996).
[2] P.E. Ulmer *et al.,* Phys. Rev. Lett. **59,** 2259 (1987).
[3] P.E. Ulmer, Ph.D. thesis, MIT (1998).
[4] R. Lourie *et al.,* Phys. Rev. Lett. **56,** 2364 (1986).
[5] R. Lourie Ph.D. thesis, MIT (1986).
[6] L. Weinstein *et al.,* Phys. Rev. Lett. **64,** 1646 (1990).
[7] L. Weinstein, Ph.D. thesis, MIT (1988).
[8] J.H. Morrison, Ph.D. thesis, MIT (1993).
[9] M.W. Holtrop, Ph.D. thesis, MIT (1995).
[10] J. Ryckebusch *et al.,* Nucl. Phys. A **624,** 581 (1997).
[11] J. Ryckebusch *et al.,* Nucl. Phys. A **476,** 237 (1988).
[12] J. Ryckebusch *et al.,* Nucl. Phys. A **503,** 694 (1989).
[13] M. Waroquier *et al.,* Phys. Rep. **148,** 249 (1987).
[14] T. Takaki, Phys. Rev. C **39,** 359 (1989).
[15] H. Muther and W.H. Dickhoff *et al.,* Phys. Rev. C **49,** R17 (1994).
[16] K. I. Blomqvist *et al.* Phys. Lett. B **344,** 85 (1995).
[17] F. Garibaldi *et al.,* Nucl. Instrum. Methods **A314,** 1 (1992).
[18] G.G. Simon *et al.,* Nucl. Phys. A **333,** 381 (1980).
[19] E. Quint, Ph.D. thesis, University of Amsterdam (1988).
[20] R. Florizone, Ph.D. thesis, MIT (1999).
[21] N. Liyanage, Ph.D. thesis, MIT (1999).
[22] J.P. Jeukenne and C. Mahaux, Nucl. Phys. A **394,** 445 (1983).
[23] J.J. Kelly, Phys. Rev. C **56,** 2672 (1997).
[24] A. Picklesimer, J. W. Van Orden, and S. J. Wallace, Phys. Rev. C**32**, 1312 (1985).
[25] A. Picklesimer and J. W. Van Orden, Phys. Rev. C**40**, 290 (1989).
[26] L. Lapikas, Nucl. Phys. A **553,** 297 (1993).
[27] W. Bertozzi, Nucl. Phys. A **527,** 347 (1991).
[28] J.B.J.M. Lanen *et al.,* Phys. Rev. Lett. **64,** 2250 (1990).
[29] G. van der Steenhoven *et al.,* Nucl. Phys. A **480,** 547 (1988).
[30] G. van der Steenhoven *et al.,* Nucl. Phys. A **484,** 445 (1988).

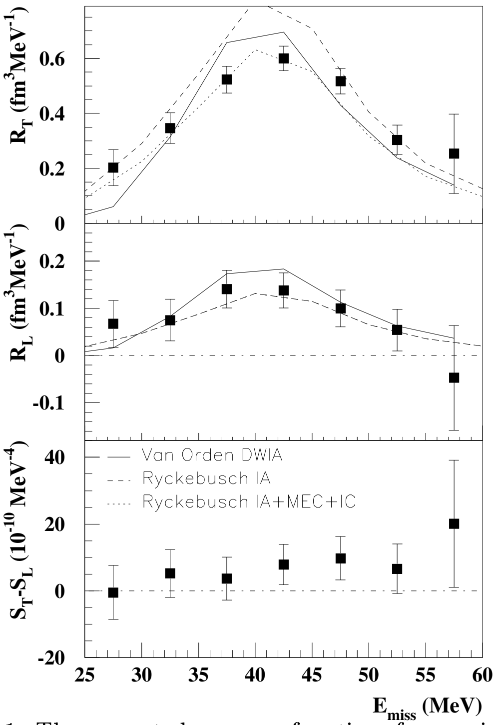

FIG. 1. The separated response functions for quasi-parallel kinematics for 45 MeV/c $< p_{miss} <$ 75 MeV/c.

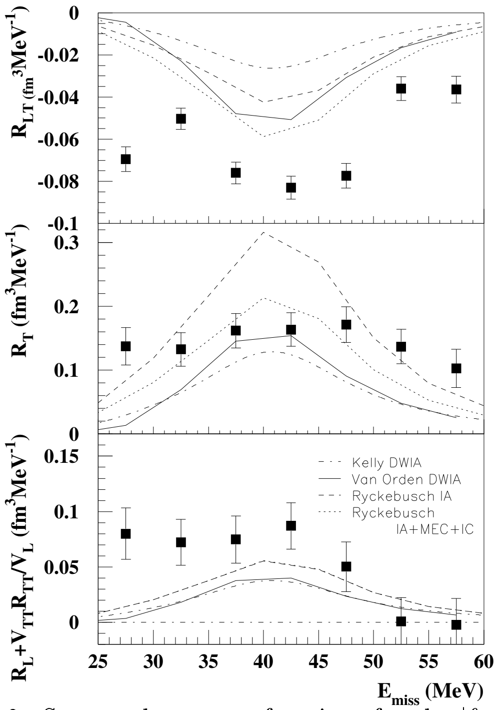

FIG. 2. Separated response functions for the $|\theta_{pq}| = 8°$ setting ($P_{miss}^{average} \approx 145$ MeV/c). Plots show (from top to bottom) R_{LT}, R_T, and $R_L + \frac{V_{TT}}{V_L} R_{TT}$.

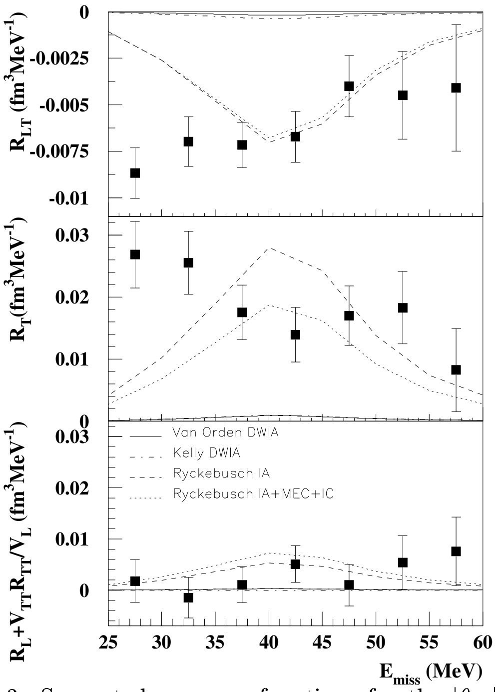

FIG. 3. Separated response functions for the $|\theta_{pq}| = 16°$ setting ($P_{miss}^{average} \approx 280.0$ MeV/c). Plots show (from top to bottom) R_{LT}, R_T, and $R_L + \frac{V_{TT}}{V_L} R_{TT}$.

E_{beam} (GeV)	θ_e (°)	θ_{pq} (°)	$\lvert\vec{p}_{miss}\rvert$ (MeV/c)
0.843	100.7	0	0
		8	140
		16	275
1.643	37.17	-8	140
		0	0
		8	140
2.442	23.38	-20	350
		-16	275
		-8	140
		0	0
		8	140
		16	275
		20	350

TABLE I. Experimental kinematics